Nanomed. J. 7(2): 149-157, Spring 2020

RESEARCH PAPER

Evaluation of protein corona formation and anticancer efficiency of curcumin-loaded zwitterionic silica nanoparticles

Shokoofeh Maghari, Alireza Ghassempour*

Department of Phytochemistry, Medicinal Plants and Drugs Research Institute, Shahid Beheshti University, Tehran, Iran

ABSTRACT

Objective(s): Study and development of antifouling nanosystem for conjugation of drugs were attracting great attention in recent years. The present study aimed to develop novel curcumin-loaded silica nanoparticles containing zwitterionic coating as an antifouling system to provide protein corona free nanoformulations for curcumin.

Materials and Methods: Silica nanoparticles were prepared using the Stöber method, and mono- and bi-functionalized nanoparticles were obtained by modifying the surface of the bare silica nanoparticles with (3-aminopropyl)triethoxysilane (APTES), polyethylene glycol amine, APTES with sulfobetaine, and polyethylene glycol amine with sulfobetaine. Nanoparticle characterization, curcumin release, and measurement of protein corona inhibition were performed after incubation in the human plasma and MTT assay to confirm the stability and efficiency of the nanoparticles.

Results: The presence of the sulfobetaine group could influence the curcumin loading capacity of the silica nanoparticles. The results of sodium dodecyl sulfate-polyacrylamide gel electrophoresis indicated no significant protein adsorption on the curcumin-loaded, zwitterionic-coated nanoparticles compared to the other nanoparticles. In addition, the MTT assay confirmed the cytotoxicity of the curcumin-loaded sulfobetaine-APTES-silica nanoparticles on MCF-7 cancer cells.

Conclusion: Our findings confirmed the effects of the zwitterionic coating on the physicochemical properties of the nanoparticles. These findings play a key role in the development of novel nanoparticles for drug delivery applications.

Keywords: *Curcumin, Functionalized Nanoparticles, Protein Corona, Silica Nanoparticles, Zwitterionic Coating*

How to cite this article

Maghari Sh, Ghassempour AR. Evaluation of protein corona formation and anticancer efficiency of curcumin-loaded zwitterionic silica nanoparticles. Nanomed J. 2020; 7(2): 149-157. DOI: 10.22038/nmj.2020.07.008

INTRODUCTION

Curcumin (CUR) is the main curcuminoid of turmeric (*Curcuma longa*) and a chemopreventive substance [1] with various pharmacological activities, such as anti-inflammatory, antioxidant, and antitumor properties [2, 3]. Moreover, CUR has demonstrated efficacy in the treatment of several malignancies, including colorectal, breast, lung, prostate, and pancreatic cancers [4].

Although CUR has various pharmacological properties, the extremely low bioavailability of this compound has limited its biomedical application [5]. The poor bioavailability of CUR has been attributed to the low gastrointestinal absorption, extensive first-pass metabolism, poor aqueous solubility, and low stability of this compound [6,7].

Several studies have been focused on developing novel formulations of CUR to improve its solubility and stability. In this regard, the conjugation of CUR with nanomaterials has recently attracted the attention of researchers [1, 8-14]. However, when nanoparticles (NPs) containing drugs enter the bloodstream, plasma proteins bind to their surfaces, forming a protein corona shield that affects the uptake and targeting efficiency of the NPs [15, 16]. Antifouling coatings such as polyethylene glycols (PEGs) could reduce the nonspecific adsorption of proteins, while hypersensitivity and degradation under stress are the major drawbacks of using these polymers for drug delivery [17]. Moreover, some plasma proteins are adsorbed to NP surfaces even in the presence of PEG coating [18, 19]. Therefore, novel

* *Corresponding Author Email: a-ghassempour@sbu.ac.ir*

Note. This manuscript was submitted on December 3, 2019; approved on February 15, 2020

antifouling systems such as zwitterionic coatings have been frequently utilized in recent years [20-22]. In addition, zwitterionic-PEG hybrids have emerged as viable options to provide stable and protein corona-free NPs [23, 24].

In the present study, the CUR loading capacity and antifouling properties of four types of mono- and bi-functionalized silica NPs were compared. Silica-based nanomaterials are widely used in biomedical approaches owing to their cost-efficient production and easy functionalization [25-27]. High CUR loading capacity has been attributed to 3-aminopropyltriethoxysilane (APTES)-functionalized poly(N-vinyl-2-pyrrolidone) fibers (28) and APTES-modified mesoporous silica NPs [29]. In the current research, bare silica NPs were synthesized using the Stöber method [30] and modified with sulfobetaine (SB), amine, and PEG alkoxysilanes. Following that, the hydrodynamic size, zeta potential, and CUR loading capacity of the mono- and bi-functionalized silica NPs were compared, and the effect of the zwitterionic system on protein adsorption to the surface of the curcumin-conjugated NPs was investigated.

MATERIALS AND METHODS

Initially, [3-(diethylamino)propyl] trimethoxysilane was purchased from TCI Development Co., Ltd. (Shanghai). All the other chemicals were provided by Sigma-Aldrich (USA). The chemicals were used as received. In addition, ultrapure deionized water (DIW) was prepared using a Milli-Q water purification system (Millipore, Bedford, MA, USA).

Instruments

The transmission electron microscope (TEM) studies were carried out using the FEI Tecnai G220 transmission electron microscope, operating at 160 or 200 kV for high-resolution imaging. Thermogravimetric analysis (TGA) was recorded on the Mettler Toledo TGA/DSC 1 STAR System at the temperature of 25-650°C with a ramp (10 K/min) in the synthetic air stream of 80 ml/min. The Fourier-transform infrared spectroscopy (FTIR) spectra were acquired in the transmission mode using the Bruker 8700 FTIR spectrometer, and UV-Vis measurements were performed using a UV-2501PC instrument (SHIMADZU). Moreover, dynamic light scattering (DLS) and ζ-potential data were measured using the Malvern Zetasizer Nano-ZS90 system, and MALDI-TOF mass spectrometry was carried out using the AB SCIEX 4800 time-of-flight (TOF/TOF) mass spectrometer in the reflectron positive ion mode, with the device equipped with a 355-nanometer Nd:YAG laser, and α-cyano-4-hydroxycinnamic acid was used as the matrix in the MALDI analysis.

Synthesis of Zwitterionic Sulfobetaine Alkoxysilane (SB)

SB was synthesized with the addition of (N,N-dimethylaminopropyl)trimethoxysilane (0.09 mmol) to 1,3-propanesultone (0.18 mmol) in dry dimethyl formamide (DMF), and refluxing was performed for 12 hours in a nitrogen atmosphere. The white precipitate product was used without additional purification.

Synthesis of Bare Silica NPs (SiO_2 NPs), APTES-modified Silica NPs (SiO_2-NH_2 NPs), SB-Silica NPs (SiO_2-SB NPs), and Thiol-PEG-Amine-modified Silica NPs (SiO_2-PEG-NH_2 NPs)

Bare silica NPs (SiO_2 NPs) with the diameter of 100 nanometers were prepared through the Stöber process. In brief, tetraethylorthosilicate (TEOS) (625 µl) was added to the mixtures consisting of methanol (10 ml), DIW (3.6 ml), and concentrated ammonia (800 µl) and stirred for six hours. Following that, the obtained NPs were centrifuged, washed, and redispersed in 10 milliliters of the DIW and ethanol mixture (ratio: 3:1). To synthesize the SiO_2-NH_2 or SiO_2-SB NPs, 20 microliters of an alkoxysilane precursor (APTES or SB) was added to the bare silica NPs and stirred for 12 hours at room temperature. The obtained NPs were lyophilized for further experimentation.

To prepare the SiO_2-PEG-NH_2 NPs, the previously lyophilized SiO_2-NH_2 NPs were dispersed in DMF and sonicated for one hour. Afterwards, 0.09 millimole of 3-(maleimido)propionic acid N-succinimidyl ester was added to the NPs, and the mixture was stirred overnight. The resulting NPs were centrifuged, and after discarding the supernatant, they were redispersed in DMF. Following that, the NH_2-PEG-SH solution (72 mg; molecular weight: 800 Dalton) was slowly added to the NPs with stirring. The pH of the mixture was set at 8.3 by the addition of the sodium hydroxide solution, and the NPs were stirred overnight in a nitrogen atmosphere. The excessive NH_2-PEG-SH was removed through the dialysis of the NPs against water. Finally, the resulting NPs were centrifuged, redispersed in DIW, and lyophilized for further analysis (Fig 1).

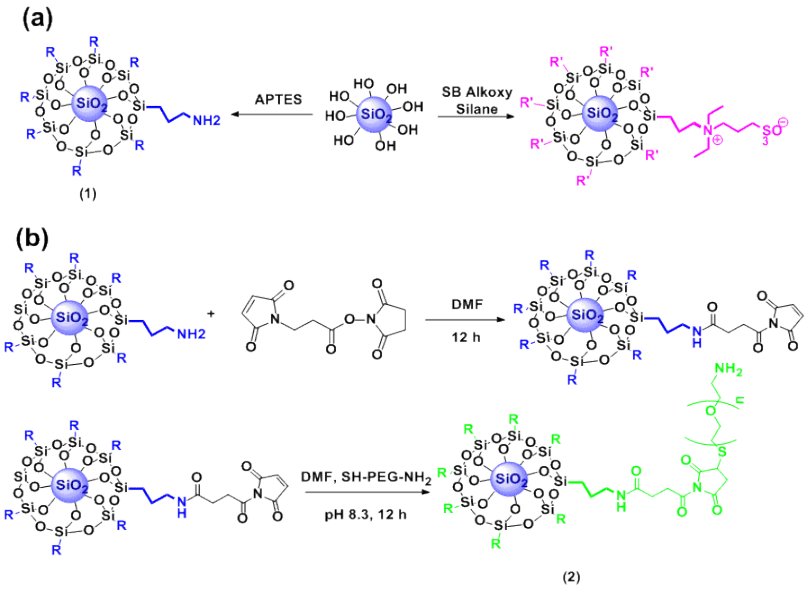

Fig 1. a) Surface Modification of SiO2 NPs with APTES and SB, b) Synthesis Pathway for Surface Modification of SiO2 NPs with SH-PEG-NH2

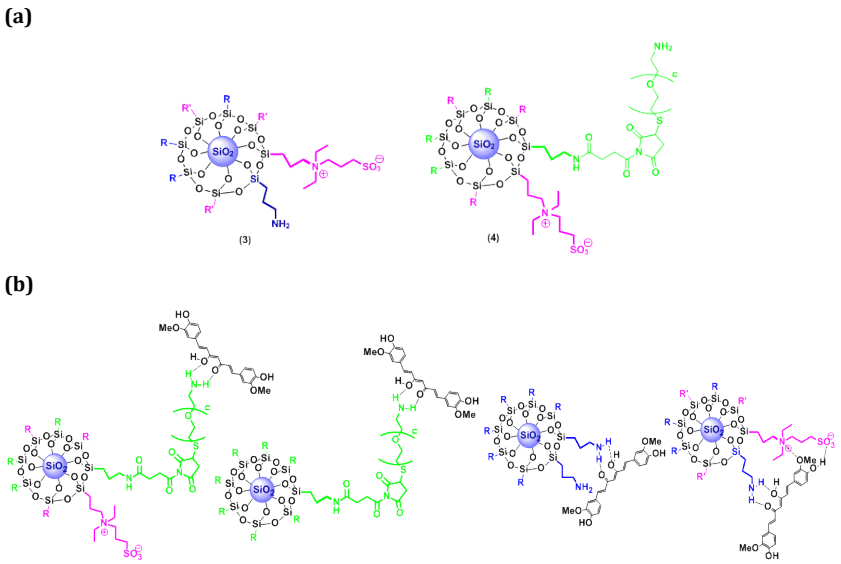

Fig 2. a) Schematic Representation of 3) SiO2-SB-NH2 and 4) SiO2-SB-PEGNH2, b) Schematic Representation of CUR-loaded Silica NPs

Synthesis of the Bi-functionalized SiO_2-SB-NH_2, and SiO_2-SB-PEG-NH_2 NPs

At this stage, the SiO_2-SB-NH_2 NPs were synthesized by adding 0.045 millimole of APTES and 0.045 millimole of the SB alkoxysilane precursor to the bare silica NPs. The mixture was stirred for 12 hours, centrifuged, and washed twice with DIW and ethanol. The same procedure was performed to prepare the SiO_2-PEG-NH_2 NPs and synthesis of the SiO_2-SB-PEG-NH_2 NPs (Fig 2).

Preparation of the CUR-loaded Silica NPs (SiO_2-NH_2-CUR, SiO_2-SB-NH_2-CUR, SiO_2-SB-PEGNH_2-CUR, and SiO_2-PEGNH_2-CUR NPs)

A solution of curcumin (2.5 mmol) in ethanol (20 ml) was added to the silica NPs, and the mixture was sonicated for six hours. The slurry was stirred at room temperature for 12 hours. Afterwards, the NPs were centrifuged and washed repeatedly with DMF in order to remove the loosely-bound CUR from the NPs. The obtained pale orange silica

NPs were dispersed in DIW for further analysis (Fig 2).

Characterization of the Synthesized Silica NPs

The FTIR, TGA, and matrix-assisted laser desorption ionization mass (MALDI-MS) analyses were performed to support the surface functionalization of the silica NPs. The size and aggregation of the free nature of the silica NPs were confirmed by TEM and DLS. Moreover, the ζ-potentials measurement of the NPs was carried out to evaluate the surface charge of the NPs.

Plasma Measurement of Protein Corona

The aqueous solutions of the bare silica NPs and all types of the CUR-conjugated silica NPs (100 µl, 1 mg/ml in DIW) were mixed with 900 microliters of the human plasma (HP) solution (50% HP in phosphate buffered saline [PBS] and 90% HP in PBS, respectively). Following that, the mixture of the NPs and HP was incubated at the temperature of 37°C and shaken for one hour. After centrifugation, the excessive HP was eliminated, and the NPs were washed with PBS twice. The NP size and zeta potential were measured before and after the incubation in the HP, and the level of the adsorbed protein by the NP surfaces were determined via gel electrophoresis.

Sodium Dodecyl Sulfate-Polyacrylamide Gel Electrophoresis (SDS-PAGE) Analysis

After the incubation of the CUR-conjugated silica NPs in the HP for one hour, the samples were washed with PBS twice, and the NPs were resuspended in protein buffer. Afterwards, the samples were boiled at the temperature of 100°C for five minutes.

At the next stage, the same volume of each sample was loaded into 12% polyacrylamide gel; the gels were run at 120 V and 80 mA for approximately 100 minutes and stained using the standard Coomassie blue protocol.

Cytotoxicity Assessment of SiO_2-SB-NH_2-CUR by the MTT Assay

MTT Assay for Free CUR and SiO2-SB

At this stage, NH_2-CUR was assessed against the MCF-7 cell line based on the reported protocol [31].

The prepared cells were treated with various concentrations of CUR and silica NPs for 48 hours. After discarding the supernatant, 120 microliters of the fresh cell culture medium was added. After one hour, 100 microliters of the MTT solution was added, and the absorbance was measured at 570 nanometers.

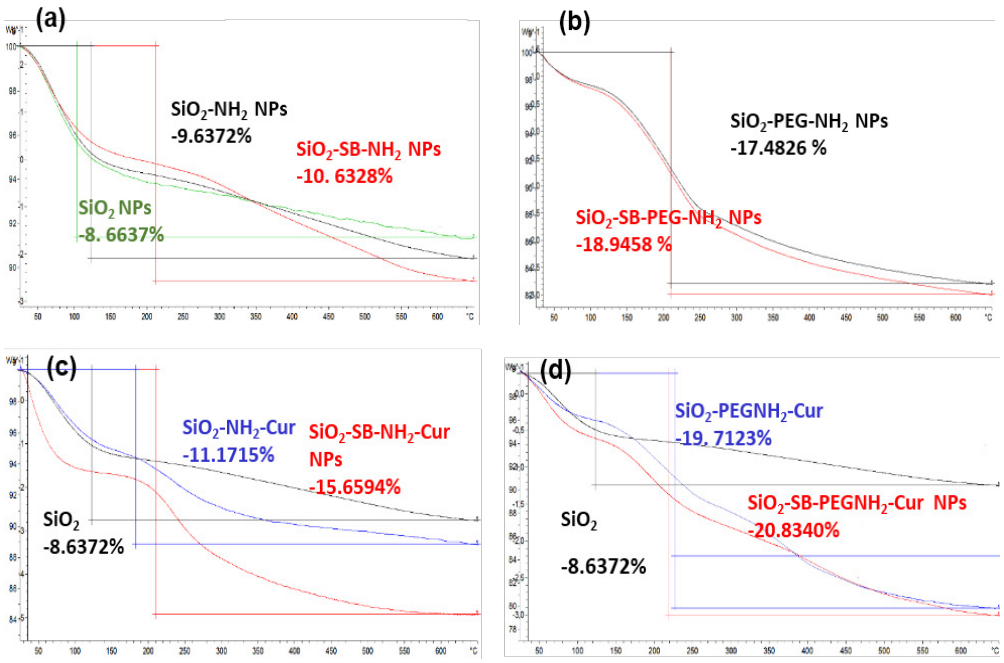

Fig 3. TGA Measurement in Silica NPs

RESULTS AND DISCUSSION

Surface Modification of the Silica NPs

According to the obtained results, the conjugation of CUR with the silica NPs could enhance CUR bioavailability due to the hydrophilic nature of the NPs. Furthermore, the use of the intermolecular hydrogen bonding interaction of the CUR carbonyl groups with the amine-functionalized nanomaterials appeared to be a promising approach to the immobilization of CUR without disrupting the therapeutic activity of the main group. The surface modification strategy is applicable to the production of effective drug delivery systems.

CUR is able to interact with various proteins through its several functional groups. The presence of an antifouling coating could prevent CUR from miss-targeting by HP proteins. As such, the SiO_2-NH_2, SiO_2-SB-NH_2, SiO_2-SB-$PEGNH_2$, and SiO_2-$PEGNH_2$ NPs were synthesized and functionalized using CUR through incubation in the CUR ethanolic solution.

In the present study, the loading capacity of the silica NPs was determined based on the TGA data (Fig 3) and by measuring the amount of the free CUR (free drug) from the total amount of the CUR (total drug) used in the preparation of the NPs (Table 1).

Table 1. TGA Results on CUR-modified Silica NPs

Type of NPs	Weight Loss Rate (25-650°C)	Curcumin (%)	Loading Capacity (%)
SiO_2-NH_2-CUR	11.1715	1.53	1.4
SiO_2-SB-NH_2-CUR	15.6594	5.02	4.61
SiO_2-$PEGNH_2$-CUR	19.7123	2.22	2.04
SiO_2-SB-$PEGNH_2$-CUR	20.8340	1.88	1.72

According to the findings, the CUR loading capacity of the SiO_2-SB-NH_2 NPs was significantly higher compared to the other NPs, which could be attributed to the effects of sulfobetaine on the improvement of the hydrogen bonding of CUR with amino silanes (Fig 2). In the SiO_2-SB-$PEGNH_2$ NPs, the difference between the size of the ligands (amino-PEG-silane and sulfobetaine-silane) prevented the simultaneous hydrogen bonding of sulfobetaine and amine groups with CUR. Therefore, the reduced number of the amine groups in the SiO_2-SB-$PEGNH_2$ NPs was compared to the SiO_2-$PEGNH_2$ NPs, which resulted in the weaker bonding of hydrogen and lower CUR loading capacity, as shown below:

$$LC\% = \frac{\text{Total Drug} - \text{Free Drug}}{\text{Weight of silica NPs}} \times 100$$

The UV-Vis absorption spectrum of the CUR-modified silica NPs indicated that the SiO_2-SB-NH_2 NPs had higher CUR compared to the other NPs (Fig 4). In addition, the MALDI-TOF mass data confirmed the presence of CUR and PEG immobilization on the surface of the silica NPs (Fig 4).

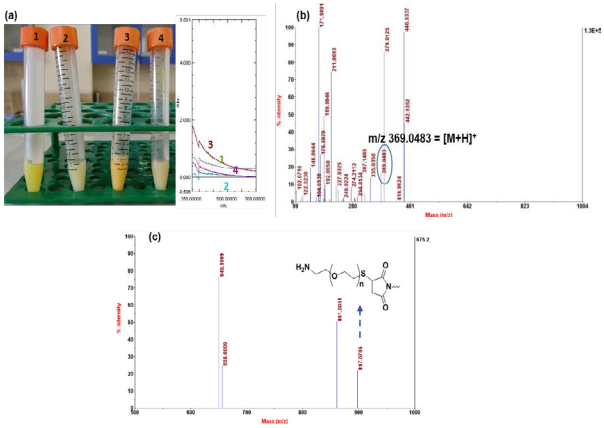

Fig 4. a) UV-Vis Spectrum of CUR-loaded Silica NPs, b) MALDI-MS Spectra of SiO2-SB-NH2-CUR (Peak at m/z 369.04 assigned to [CUR+H]+(C) MALDI-MS spectra of SiO2-PEGNH2; peak at m/z 897.07 related to [C9H16N2O3S+H]+ fragment ion)

Fig 5 depicts the FTIR spectra of the CUR-conjugated silica NPs. Accordingly, the increased intensity of the characteristic C-H stretching vibrations at 2850-2950 cm^{-1}, O-H stretching vibrations at 3422 cm^{-1}, and C=O stretching vibrations at 1632 cm^{-1} ascribed to the loaded CUR after the surface treatment of the NPs. Furthermore, SiO_2-SB-NH_2-CUR and SiO_2-$PEGNH_2$-CUR showed higher peak intensities in relation to CUR compared to the other NPs.

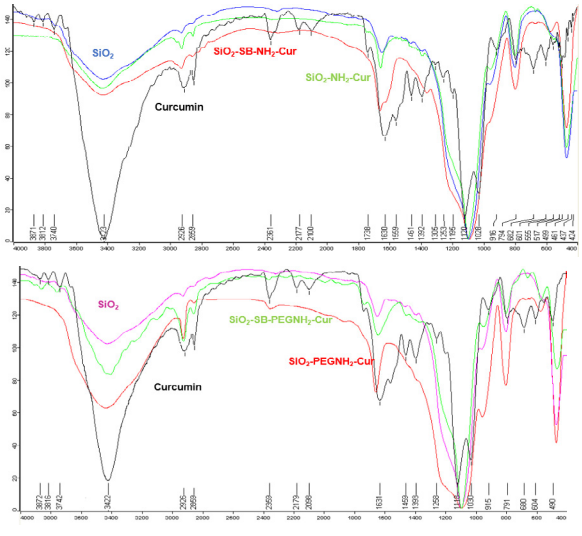

Fig 5. FTIR Spectrum of Silica NPs

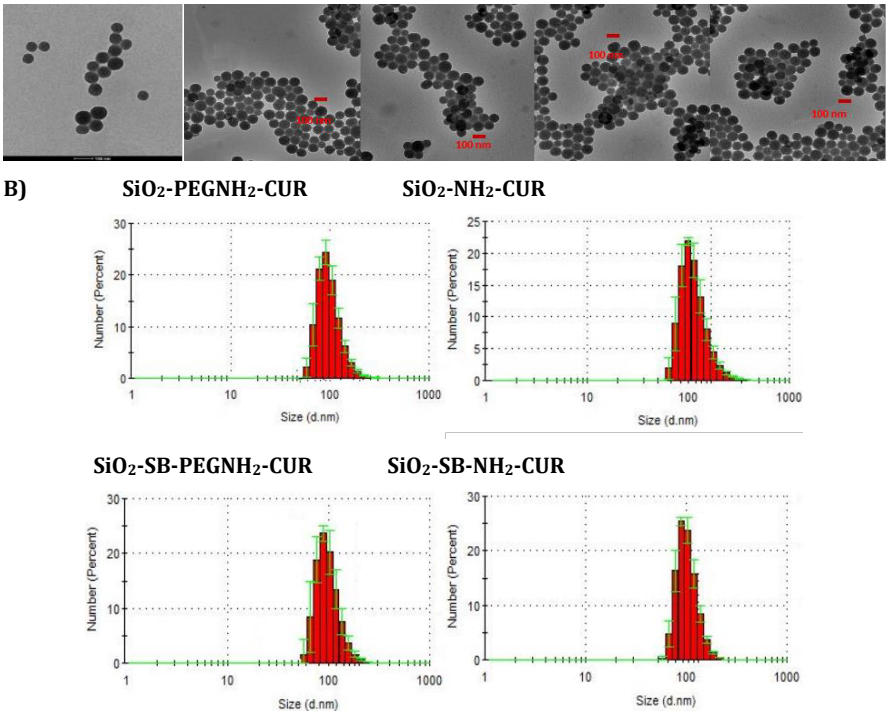

Fig 6. A) TEM and B) DLS Data of Modified Silica NPs

Fig 6. A) TEM and B) DLS Data of Modified Silica NPs

Type of NPs		Size [Dh], (nm)	potential
SiO_2-NH_2-Cur	DIW	120 ± 1.1	-0.95 ± 0.8
	HP 50%	135 ± 8.3	-30.5 ± 2.4
	HP 90%	180 ~ 350	-45.3 ± 1.6
SiO_2-SB –NH_2-Cur	DI	110 ± 3.2	-8.5 ± 0.4
	HP 50%	113 ± 1.3	-9.1 ± 0.6
	HP 90%	115 ± 1.2	-9.7 ± 1.3
SiO_2-$PEGNH_2$-Cur	DI	109 ± 4.1	-0.2 ± 1.2
	HP 50%	110 ± 2.3	-10.3 ± 1.7
	HP 90%	114 ± 1.2	-16.8 ± 1.1
SiO_2-SB –$PEGNH_2$-Cur	DI	112 ± 1.4	-7.4 ± 0.9
	HP 50%	112 ± 1.7	-9.2 ± 0.4
	HP 90%	114 ± 3.2	-9.6 ± 0.2

According to the TEM and DLS data, the surface functionalization of the silica NPs had no signs of NP aggregation (Fig 6; Table 2). As is shown in Fig 7, the silica NPs were stable at various concentrations of PBS.

SiO_2-NH_2-CUR NPs with no zwitterionic/PEG coating had significant changes in the particle diameter.

According to the information in Table 2, the coating of the NP surfaces with PEG and zwitterionic sulfobetaine prevented the aggregation of the NPs and protein adsorption after incubation in the HP.

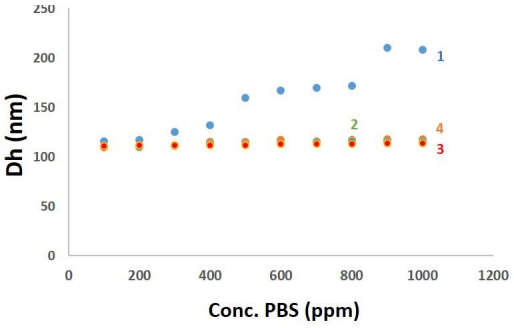

Fig 7. DLS of Silica NPs after Incubation in Various Concentration of PBS

On the other hand, the increase size of the SiO_2-NH_2-CUR NPs in the HP resulted from the instability of the modified NPs and interaction with proteins.

The surface zeta potential measurements indicated that the surface charge of the zwitterionic-coated NPs did not change significantly after incubation in the HP (Table 2), which confirmed the antifouling properties of the zwitterionic-modified silica NPs.

Measurement of the Interactions of the CUR-functionalized Silica NPs with HP Using SDS-PAGE

After the incubation of the CUR-modified silica NPs in the HP, gel electrophoresis was performed, and a significant difference was observed in the protein adsorption of the silica NPs.

Furthermore, CUR could interact with proteins variably.

Therefore, the SiO_2-NH_2-CUR NPs could adsorb more plasma protein compared to the bare silica NPs, which resulted from the trapping of the plasma proteins by CUR.

On the other hand, the SiO_2-SB-NH_2-CUR NPs resulted in light protein bands in the SDS-PAGE, confirming the key role of SB in protein corona inhibition (Fig 8).

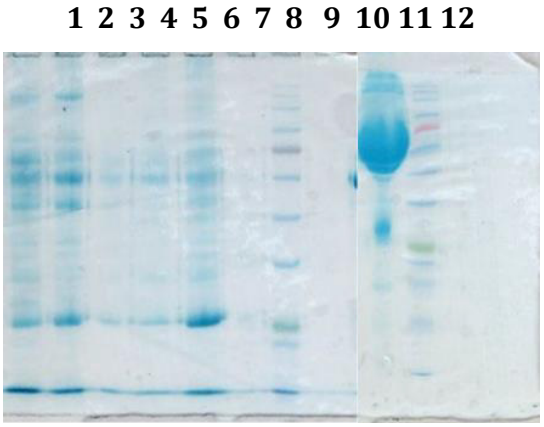

Fig 8. SDS-PAGE Gel for Silica NPs after Incubation in HP (50% and 90%) (Represented protein bands related to 1) 50% SiO2-NH2-CUR, 2) 90% SiO2-NH2-CUR, 3) 50% SiO2-SB-NH2-CUR, 4) 90% SiO2-SB-NH2-CUR, 5) bare silica, 6) 90% SiO2-PEGNH2-CUR, 7) ladder, 8) 50% SiO2-PEGNH2-CUR, 9) HP, 10) ladder, 11) 50% SiO2-SB-PEGNH2-CUR, 12) 90% SiO2-SB-PEGNH2-CUR)

The SiO_2-SB-PEGNH_2-CUR NPs showed no adsorbing protein bands.

The results of the SDS-PAGE indicated that the simultaneous use of PEG and zwitterionic coatings could enhance the antifouling properties of the NPs, which supported the DLS and zeta potential data in the previous section.

The antifouling properties of the zwitterionic coating resulted from the highly hydrated layer that was formed by the electrostatic force.

This layer was stronger than the hydration layer formed by the hydrogen bonding of PEG.

However, the presence of PEG reduced the electrostatic repulsion of the zwitterionic moieties, and the synergistic effect was observed when these coatings were used together.

CUR Release

The CUR release profiles in PBS (7.4) are depicted in Fig 9.

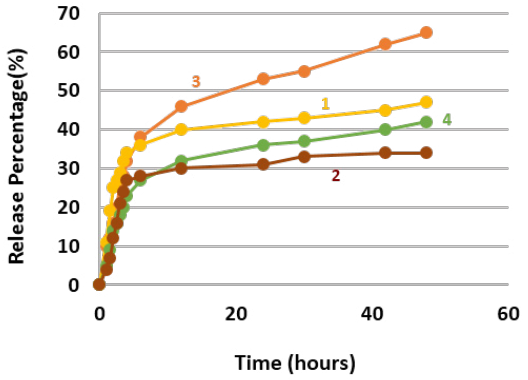

Fig 9. CUR-loaded Silica NP Release Profiles; 1) SiO2-SB-PEGNH2-CUR NPs, 2) SiO2-SB-NH2-CUR, 3) SiO2-NH2-CUR, 4) SiO2-PEGNH2-CUR

According to the findings, the CUR-modified silica NPs exhibited the rapid release of more than 50% within 12 hours.

The comparison of CUR release patterns indicated that the release of CUR from the SiO_2-SB-NH_2 NPs was slightly slower than the SiO_2-PEG-NH_2 NPs, which confirmed the stronger binding of CUR with the NP surfaces.

MTT Assay

To evaluate the cytotoxicity of the SiO_2-SB-NH_2-CUR, the MCF-7 cell line was selected in the present study.

The measurement of the IC_{50} values for the free CUR and SiO_2-SB-NH_2-CUR NPs revealed the higher toxicity of the silica NPs (~10%) without affecting the normal cells.

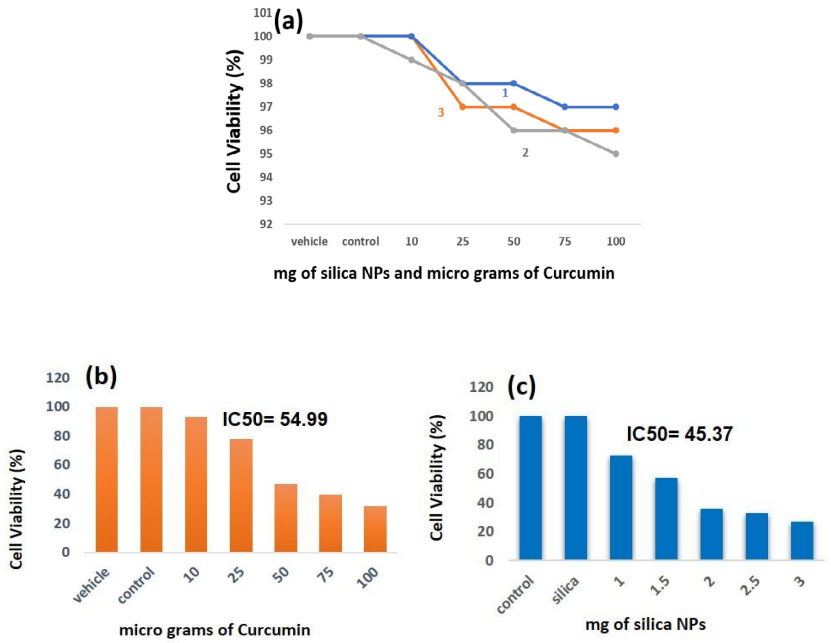

Fig 10. Cytotoxicity of a, 1) Bare Silica NPs, 2) SiO2-SB-NH2-CUR NPs, 3) CUR on Fibroblast Cell Line (IMR-90); b) Free CUR on MCF-7 Cell Line; c) SiO2-SB-NH2-CUR NPs on MCF-7 Cell Line

CONCLUSION

In the present study, we demonstrated the design of four types of modified silica NPs and their conjugation with CUR. According to the findings, the presence of zwitterionic sulfobetaine on the surface of the silica NPs could significantly improve the CUR loading capacity, as well as the antifouling properties of the modified NPs. In addition, the combination of PEG and zwitterionic ligand had positive effects on the repellent properties of protein in the NPs. Furthermore, the MTT assay of the breast cancer cell lines confirmed the cytotoxicity of the CUR-conjugated silica NPs. These findings are essential to the development of more efficient drug delivery systems in the future.

ACKNOWLEDGMENTS

Hereby, we extend our gratitude to the Iranian National Science Foundation (INSF) for the financial support of this research project (code: 96003475).

REFERENCES

1.Falconieri M, Adamo M, Monasterolo C, Bergonzi M, Coronnello M, Bilia A. New Dendrimer-Based Nanoparticles Enhance Curcumin Solubility. Planta Med. 2016; 22; 83(05): 420–425.

2.Gomes CA, Girão da Cruz T, Andrade JL, Milhazes N, Borges F, Marques MPM. Anticancer Activity of Phenolic Acids of Natural or Synthetic Origin: A Structure–Activity Study. J Med Chem. 2003; 46(25): 5395–5401.

3.Chakraborti S, Dhar G, Dwivedi V, Das A, Poddar A, Chakraborti G, Basu G, Chakrabarti P, Surolia A, Bhattacharyya B. Stable and Potent Analogues Derived from the Modification of the Dicarbonyl Moiety of Curcumin. Biochemistry. 2013; 52(42): 7449–7460.

4.Yang X, Li Z, Wang N, Li L, Song L, He T, Sun L, Wang Z, Wu Q, Luo N, Yi C. Curcumin-Encapsulated Polymeric Micelles Suppress the Development of Colon Cancer In Vitro and In Vivo. Sci Rep. 2015; 5(1): 10322.

5.Siviero A, Gallo E, Maggini V, Gori L, Mugelli A, Firenzuoli F, Vannacci A. Curcumin, a golden spice with a low bioavailability. Journal of Herbal Medicine. 2015; 5(2): 57–70.

6.Hsu C-H, Cheng A-L. CLINICAL STUDIES WITH CURCUMIN. In: Aggarwal BB, Surh Y-J, Shishodia S, editors. The Molecular Targets and Therapeutic Uses of Curcumin in Health and Disease Boston, MA: Springer US; 2007, p. 471–480. Available from: http://link.springer.com/10.1007/978-0-387-46401-5_21

7.Anand P, Kunnumakkara AB, Newman RA, Aggarwal BB. Bioavailability of Curcumin: Problems and Promises. Mol Pharmaceutics. 2007; 4(6): 807–818.

8.Thu Huong LT, Nam NH, Doan DH, My Nhung HT, Quang BT, Nam PH, Thong P.Q, Phuc N.X, Thu H.P. Folate attached, curcumin loaded Fe3O4 nanoparticles: A novel multifunctional drug delivery system for cancer treatment. Materials Chemistry and Physics. 2016; 172: 98–104.

9.Magro M, Campos R, Baratella D, Lima G, Holà K, Divoky C, Stollberger R, Malina O, Aparicio C, Zoppellaro G, Zbořil R. A Magnetically Drivable Nanovehicle for Curcumin with Antioxidant Capacity and MRI Relaxation Properties.

Chem Eur J. 2014; 20(37): 11913–11920.
10.Manju S, Sharma CP, Sreenivasan K. Targeted coadministration of sparingly soluble paclitaxel and curcumin into cancer cells by surface engineered magnetic nanoparticles. J Mater Chem. 2011; 21(39): 15708.
11.Yallapu MM, Ebeling MC, Khan S, Sundram V, Chauhan N, Gupta BK, Puumala SE, Jaggi M, Chauhan SC. Novel Curcumin-Loaded Magnetic Nanoparticles for Pancreatic Cancer Treatment. Molecular Cancer Therapeutics. 2013; 12(8): 1471–1480.
12.Nh G, Li J. Targeted Theranostic Approach for Glioma Using Dendrimer-Based Curcumin Nanoparticle. J Nanomed Nanotechnol. 2016; 7(4). https://www.omicsonline.org/open-access/targeted-theranostic-approach-for-glioma-using-dendrimerbasedcurcumin-nanoparticle-2157-7439-1000393.php?aid=77685
13.Pillai JJ, Thulasidasan AKT, Anto RJ, Devika NC, Ashwanikumar N, Kumar GSV. Curcumin entrapped folic acid conjugated PLGA–PEG nanoparticles exhibit enhanced anticancer activity by site specific delivery. RSC Adv. 2015; 5(32): 25518–25524.
14.Salem M, Xia Y, Allan A, Rohani S, Gillies ER. Curcumin-loaded, folic acid-functionalized magnetite particles for targeted drug delivery. RSC Adv. 2015; 5(47): 37521–37532.
15.Lynch I, Dawson KA. Protein-nanoparticle interactions. Nano Today. 2008; 3(1–2): 40–47.
16.Salvati A, Pitek AS, Monopoli MP, Prapainop K, Bombelli FB, Hristov DR, Kelly PM, Åberg C, Mahon E, Dawson KA. Transferrin-functionalized nanoparticles lose their targeting capabilities when a biomolecule corona adsorbs on the surface. Nature Nanotech. 2013; 8(2): 137–143.
17.Efremova NV, Sheth SR, Leckband DE. Protein-Induced Changes in Poly(ethylene glycol) Brushes: Molecular Weight and Temperature Dependence. Langmuir. 2001 ; 17(24): 7628–7636.
18.Kim HR, Andrieux K, Delomenie C, Chacun H, Appel M, Desmaële D, Taran F, Georgin D, Couvreur P, Taverna M. Analysis of plasma protein adsorption onto PEGylated nanoparticles by complementary methods: 2-DE, CE and Protein Lab-on-chip® system. Electrophoresis. 2007; 28(13): 2252–2261.
19.Pozzi D, Colapicchioni V, Caracciolo G, Piovesana S, Capriotti AL, Palchetti S, De Grossi S, Riccioli A, Amenitsch H, Laganà A. Effect of polyethyleneglycol (PEG) chain length on the bio–nano-interactions between PEGylated lipid nanoparticles and biological fluids: from nanostructure to uptake in cancer cells. Nanoscale. 2014; 6(5): 2782.
20.Estephan ZG, Schlenoff PS, Schlenoff JB. Zwitteration As an Alternative to PEGylation. Langmuir. 2011; 27(11): 6794–6800.
21.Estephan ZG, Jaber JA, Schlenoff JB. Zwitterion-Stabilized Silica Nanoparticles: Toward Nonstick Nano. Langmuir. 2010; 26(22): 16884–16889.
22.Safavi-Sohi R, Maghari S, Raoufi M, Jalali SA, Hajipour MJ, Ghassempour A, Mahmoudi M. Bypassing Protein Corona Issue on Active Targeting: Zwitterionic Coatings Dictate Specific Interactions of Targeting Moieties and Cell Receptors. ACS Appl Mater Interfaces. 2016; 8(35): 22808–22818.
23.Huang J, Xu W. Zwitterionic monomer graft copolymerization onto polyurethane surface through a PEG spacer. Applied Surface Science. 2010; 256(12): 3921–3927.
24.Liu J, Xu T, Gong M, Yu F, Fu Y. Fundamental studies of novel inorganic–organic charged zwitterionic hybrids. Journal of Membrane Science. 2006; 283(1–2): 190–200.
25.Xie M, Shi H, Ma K, Shen H, Li B, Shen S, Wang X, Jin Y. Hybrid nanoparticles for drug delivery and bioimaging: Mesoporous silica nanoparticles functionalized with carboxyl groups and a near-infrared fluorescent dye. Journal of Colloid and Interface Science. 2013; 395: 306–314.
26.Wu X, Wu M, Zhao JX. Recent development of silica nanoparticles as delivery vectors for cancer imaging and therapy. Nanomedicine: Nanotechnology, Biology and Medicine. 2014; 10(2): 297–312.
27.He Q, Shi J. Mesoporous silica nanoparticle based nano drug delivery systems: synthesis, controlled drug release and delivery, pharmacokinetics and biocompatibility. J Mater Chem. 2011; 21(16): 5845.
28.Kurniawan A, Gunawan F, Nugraha AT, Ismadji S, Wang M-J. Biocompatibility and drug release behavior of curcumin conjugated gold nanoparticles from aminosilane-functionalized electrospun poly(N -vinyl-2-pyrrolidone) fibers. International Journal of Pharmaceutics. 2017; 516(1–2): 158–169.
29.Kotcherlakota R, Barui AK, Prashar S, Fajardo M, Briones D, Rodríguez-Diéguez A, Patra CR, Gómez-Ruiz S. Curcumin loaded mesoporous silica: an effective drug delivery system for cancer treatment. Biomater Sci. 2016; 4(3): 448–459.
30.Stöber W, Fink A, Bohn E. Controlled growth of monodisperse silica spheres in the micron size range. Journal of Colloid and Interface Science. 1968; 26(1): 62–69.
31.Kong Z-L, Kuo H-P, Johnson A, Wu L-C, Chang KLB. Curcumin-Loaded Mesoporous Silica Nanoparticles Markedly Enhanced Cytotoxicity in Hepatocellular Carcinoma Cells. IJMS. 2019; 20(12): 2918.